



The Open Atmospheric Science Journal

Content list available at: www.benthamopen.com/TOASCJ/

DOI: 10.2174/1874282301711010121



RESEARCH ARTICLE

MODIS Summer SUHI Cross-sections Anomalies over the Megacities of the Monsoon Asia Region and Global Trends

Hofit Itzhak-Ben-Shalom^{1,*}, Pinhas Alpert², Oded Potchter^{3,4} and Rana Samuels²¹The Porter School of Environmental Studies, Tel Aviv University, 69978 Tel Aviv, Israel²Department of Geosciences, Tel-Aviv University, P.O. Box 39040, Tel Aviv, Israel³Department of Geography and the Human Environment, Tel Aviv University, Tel Aviv, Israel⁴Department of Geography, Beit Berl College, Beit Berl, Israel

Received: August 16, 2017

Revised: August 21, 2017

Accepted: October 02, 2017

Abstract:

Background:

Evidence has accumulated in recent years regarding the scope of local and global climate changes attributed to exacerbating anthropogenic factors such as accelerating population growth, urbanization, industrialization, traffic and energy use. Remote space monitoring, unlike ground-based measurements, has the advantage of providing global coverage on a daily basis.

Methods:

MODIS (Moderate Resolution Imaging Spectroradiometer) Aqua and Terra 1°×1° spatial resolution as well as the 1 km higher resolution of Aqua-MODIS were investigated for a global overview of megacities temperature variations, as well as the recent trends of the 10 largest Monsoon Asian megacities.

Results:

The average Land Surface Temperature (LST) cross-sections of the 10 Asian megacities were examined for June-August 2002-2014. Temperature variations fit a spatial bell-shaped curve, with a pronounced maximum over the city center. Nighttime data indicated sharp LST decreases with distance from the city center, particularly in the coldest cities, those of Tokyo, Seoul, Osaka and Beijing.

Conclusion:

Daytime latitudinal (E-W) and longitudinal (N-S) Surface Urban Heat Islands (SUHI) have steeper gradients than for nighttime data. During daytime, the SUHI gradients are largest in Tokyo, Seoul, Osaka and Beijing with values reaching 15°C followed by the cities of Shanghai and Guangzhou with ~11°C, and Karachi with ~5°C SUHI. Nighttime SUHIs were more moderate, 4-6°C in Tokyo, Seoul ~5°C, Osaka 5-7°C and Beijing ~7°C. Only in the three largest megacities, *i.e.*, Tokyo, Guangzhou and Shanghai, did the nighttime LST trends decline.

Keywords: Surface Urban Heat Island (SUHI), Megacities, Space monitoring, Terra- and Aqua-MODIS, Climate change, Temperature, Population.

1. INTRODUCTION

50% of the world's population now lives in cities, with this percentage projected to increase [1]. Urban areas with populations exceeding 10 million inhabitants are known as megacities; and such large concentrated populations have been identified as a major environmental issue, especially in developing countries [2]. Although cities occupy a small

* Address correspondence to this author at the The Porter School of Environmental Studies, Tel Aviv University 69978, Tel Aviv, Israel, Tel: 972-524-550040; E-mail: hofitben@gmail.com

fraction of land, amounting to only 2.8 per cent of the Earth's land area [3], they are considered to have indirectly triggered global climate change due to their insatiable appetite for energy and materials [4]. Alpert *et al.* [5], for instance, found that in megacities, which tend to have high levels of aerosol emissions, the Aerosol Optical Depth (AOD) indicates significantly increasing levels of anthropogenic pollution. Furthermore, rapidly expanding cities, as major consumers of energy and materials, have deteriorating air quality, as population, traffic, energy use, and industrialization grow [2, 6, 7]. Fossil fuels are consumed due to large vehicular populations. Given their very high population densities and high-rise buildings, cities also absorb a greater amount of solar radiation. Seven of the 10 most populous countries in the world – China, India, Indonesia, Russia, Pakistan, Bangladesh and Japan – are located in Asia [8].

The Asian region is marked by continuing high-level emissions of greenhouse gases from human activities [9]. IPCC Global Climate Models (GCMs) predict that the increase in annual mean warming could reach about 3°C by the 2050s and about 5°C by the 2080s over selected regions in Asia [4]. A recent study using a Regional Climate Model (RCM) found that by the end of this century Southwest Asia will be uninhabitable [10, 11].

In light of the burgeoning population, social environment scientists and policy makers have recently begun to take special notice of urban climate change [12, 13]. Various studies have also argued that significant collaboration between city planners and climate change scientists is required if these areas are to continue to maintain their livability and reduce their effect on global climate change [14 - 19].

Until recently, research on urban warming and its links to regional as well as global warming has been limited to observational measurements taken in mature cities, the only sites providing good sources of the data required for interpreting trends in urban climate change [20]. These in situ data have the advantage of long-term records but the disadvantage of poor spatial resolution [21 - 24]. More recently, observation from satellites, one of the most novel and effective monitoring tools developed for recording temperature change phenomena [25] over broad geographic areas has come into use due to its methodological efficacy in recording local information [4].

Land surface temperature (LST) plays a significant feature of global temperature [20]. The field of remote sensing lends itself well to urban climatology studies due to its greatly improved spectral and spatial resolution, which facilitates tracking the development of the respective phenomena [26]. The advantage it provides in measuring LST as a feature of global temperature has been noted in several studies that have focused on individual urban areas in China [27 - 30], India [31], and Dubai [32].

Recent studies have linked change in LST with atmospheric circulation; see for example, Zhuo [33] in China and Zhou and Wang [34] over global deserts. Lensky and Dayan [35] attempted to quantify the impact of several atmospheric circulations on LST patterns over the Eastern Mediterranean for 2000–2012 MODIS data. They found that the differences between the LST data retrieved from satellites and 2-m air temperature data as reported by land-based meteorological stations generally increase with stronger sun insolation but decline with the turbulence caused by strong winds. These parameters also vary according to synoptic-scale circulation, which is affected by horizontal pressure gradients and cloud cover. Lensky and Dayan [35] have shown that synoptic circulation induces LST patterns, with variations in LST related, among others, to vegetation cover, clouds, water vapor, surface heterogeneity, and topography [36]. In another study, Lensky and Dayan [37] found that the high spatial variability of surface temperatures induces similar variability in 2-m air temperatures, hampering representation of these temperatures in numerical models [38]. As LST differs from 2-m air temperature in terms of physical magnitude, the derivation of 2-m air temperatures from LSTs is not straightforward [39].

In consequence, methods applying statistical approaches and spatial smoothing are employed when predicting air temperatures from LSTs even though the outcomes are applicable only to the domain for which they were developed [40, 41] and are sensitive to station density [42]. Although Blandford [43] adopted a physical approach using surface data at different altitudes to retrieve the thermal profile of the ~1500 m boundary layer, this method is unable to detect near-surface (2-m) temperatures.

In the last 2-3 decades, the number of comparative studies using satellite data has grown, with the technology allowing coverage of large geographic areas, thereby creating new opportunities for climate change research [20]. Imhoff [44], for example, examined the LST data obtained from MODIS for an average of three years (2003-2005) in the 38 most populous cities in the United States. The results demonstrated that Urban Heat Island (UHI) amplitude increases with city size and is seasonally asymmetric at a large number of sites. Peng [45] selected 428 of the world's largest cities when exploring the global drivers of the Surface Urban Heat Island (SUHI). Jin and Dickinson [39],

analyzed the MODIS skin temperature observations during 9 years (2000-2009) for diurnal, seasonal, and inter-annual variations at a 0.05° latitude/longitude grid over the global land surface. In 2010, Clinton and Gong [14] performed a composite Aqua and Terra -MODIS analysis (with 5- and 10-km buffers) of the factors influencing urban vs. rural SUHI temperatures, followed by its global analysis and ranking of the urban areas surveyed. Both studies mapped urban areas while here the focus is given to the individual megacities in Asia. Also, extending time series longer-term LST trends (2002-2012) as they appeared in all the world's megacities are investigated here, in an effort to explain the inter-megacity variations. Tran *et al.* [20] also employed a 1-km MODIS resolution for 2001-2003 in their study of the SUHI's spatial patterns for eight Asian megacities as well as its relationship to land-cover properties such as vegetation, population and city area. While here, the 1-km MODIS resolution was employed when investigating longer-term LST trends (2003-2014) over the world's 29 largest megacities (>10 million inhabitants). It should be noticed that there are many more studies of the UHI of individual cities that are not cited here.

The overall objective of this study is to provide local comparative cross-sectional data of the SUHI for the top 10 megacities in the Monsoon Asian Region, the world's most rapidly growing geographic area. A further goal, for global comparison, was to provide an overview of trends in global temperature changes for 29 megacities based on MODIS LST data retrievals. In addition, comparisons between LST trends with different MODIS resolutions, *i.e.*, 1 deg and 1 km, available in the Monsoon Asian Region, were also conducted.

2. MATERIAL AND METHODS

2.1. Data Sets

2.1.1. Population Data

For the purpose of this study, we defined global megacities as such with populations exceeding 10 million, based on Brinkhoff's recommendations [46]. Agglomerations include a central city and neighboring communities, linked to the central city by either continuous built-up areas or a predetermined number of commuters. Some agglomerations may have two or more central cities (*e.g.*, The Ruhr) although the majority have only one. Countries, cities, population and latitude-longitude coordinates appear in (Table 1 and Fig. 1).

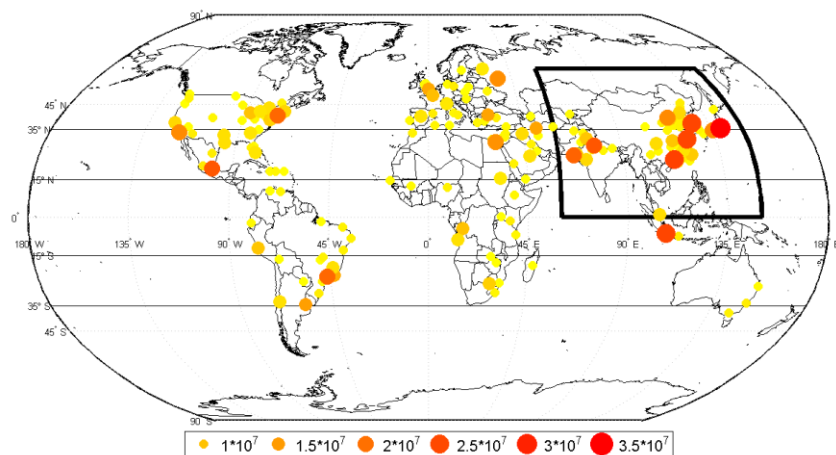


Fig. (1). Global distribution of population (2010), over the world's 233 largest cities (population exceeding 2 million). The largest cities in the Monsoon Asian Integrated Region are in bold. Population magnitude is designated by circles of different diameters and colors, as elaborated in the bottom panel.

2.1.2. MODIS Data

MODIS, the Moderate Resolution Imaging Spectroradiometer, is a satellite programmed to collect data for the spatial and temporal characteristics of the global LST during daytime and nighttime [47]. The monitor has 36 channels, spanning the spectral range of 0.41 to 15 μm . MODIS, with its 2330-km viewing swath, provides almost daily global coverage. We employed Collection 5 (MOD08_M3.050) of Terra -MODIS and Collection 5.1 of Aqua -MODIS

(MYD08_M3.051) level-3 monthly data with a global $1^{\circ} \times 1^{\circ}$ grid for the summer months - June to August – for the ten-year period 2002-2012.

An Aqua and Terra - MODIS database was constructed to enable estimation of LST trends. Global and local overviews in specific megacities were obtained using the two aforementioned sensors, positioned aboard two NASA satellites: Terra (launched in December 1999) and Aqua (launched in May 2002). With cameras focused directly (straight down) at the earth's surface, MODIS technology records a broad range of global temperature and other data. The LST trends themselves were calculated for the summer months, when data from the two sensors were available [48 - 51].

2.1.3. Cloudiness Effect

The MODIS expanse becomes limited with increasing cloud cover [52, 53] due to the aerosol effect. This means that the satellite's data retrieval under overcast conditions is less accurate than when cloud cover is nonexistent or thin due to aerosols. According to Remer *et al.* [52, 53], percent cloud cover exceeding 0.8, may lead to overestimated satellite retrieval of AOD because cloud droplets can become mixed with coarse mode particles. In order to minimize retrieval uncertainty, the data used was collected only during months characterized by percent cloud cover below 0.7. The effect of cloudiness on land surface temperature may be significantly smaller (personal communication with MODIS people) still the present analysis screened high-cloudiness months. It is assumed that this screening did not have a significant influence on our SUHI results.

2.1.4. The MODIS 8-Day 1-km LST

Products in the Giovanni cover the Monsoon Asian Integrated Regional Study (MAIRS) region [50]. The 8-day product's observation time is a simple average of daily observation time. Terra's daily local equator-crossing times are 10:30 AM and 10:30 PM, whereas Aqua's daily passes occur at local 1:30 AM and 1:30 PM. Orbit width is 2,330 km; hence, local time at its edge indicates a difference of approximately 1.5 hours. For the SUHI investigation we focused only on Aqua -MODIS data to ensure that the satellite sensors could differentiate between LST trends over megacities and the surrounding rural areas at 1:30 PM, the hottest hour of the day. The subsequent data file, which covers the entire Asian Monsoon Region, was comprised of averaged daytime and nighttime LSTs under cloudless conditions, with quality flags, during the summer months June to August, 2003-2014.

It should be clarified that the Terra and Aqua -MODIS readings obtained to extract trends and mean LST data have two different resolutions; first, $1^{\circ} \times 1^{\circ}$ (summer 2002-2012), for the world's 233 largest cities and second employing the finer 1 km horizontal grid (summer 2002-2014), for the 10 megacities in the Asian Monsoon Region. In addition, it was assumed here that the detectable temperature differences and/or absolute temperature accuracies of the MODIS sensor had a small effect on the calculated trends. This, because changes in the MODIS sensor accuracy during the 11-12 years period were assumed to be small enough.

3. METHODOLOGY

3.1. Temperature Analysis

Our approach to estimating the effect of urbanization on temperature change across the world's top ten megacities was based on an analysis of long-term variations in LST trends for the chosen sites in the selected time period. The LST parameters estimated in three stages. First, we investigated the latitudinal and longitudinal spread of each city center and confirmed our results with Google Earth. In order to compare mean LST distributions between city centers, mean LST values, labeled “running mean”, acted as a filter for the calculated vectors as follows in Equation (1):

$$(1) Y(i) = \text{sum}(X(j)) / (2 * M + 1), \text{ for } j = (i - M) : (i + M), \text{ and } i = 1 : \text{length}(X)$$

Where $Y = \text{RUNMEAN}(X, M)$ calculates a running mean on the elements of vector X , which in this study is the LST Average, using a window of $2 * M + 1$ data points. M is defined as the length of each city's vector for each city's latitudinal and longitude distribution.

In the second stage, we created a global map at $1^{\circ} \times 1^{\circ}$, day and night, covering the world's 233 largest cities (*i.e.*, population exceeding 2 million), including the world's 29 megacities, based on the Terra and Aqua -MODIS readings obtained during the study period (summer 2002-2012). To ensure that the satellite sensors would differentiate between LST trends in megacities and the surrounding rural areas, we used Aqua -MODIS (1 km resolution) data exclusively.

The 1 km resolution is better for understanding the impact of urbanization on local climate. The Aqua data are available for 10 megacities in the Asian Monsoon Region (counted among the world's 20 largest cities) during June-August, 2003-2014. It should note that cloudiness impedes data collection in tropical climates during the rainy season. Hence, no data is available for India among other sites. In addition, megacities for which more than six years of data were missing were deleted from the sample in order to minimize retrieval uncertainty.

3.2. Study Area

The Asian Monsoon Region extends from 0° to 60°N, 60° to 150°E; it includes eastern China, the Japanese islands, the Korean peninsula, Mongolia, Taiwan (Republic of China), Pakistan and India. Geographically, the region is located in the eastern segment of the Eurasian continent — the world's largest continent — and borders the Pacific, the world's largest ocean [4]; (Fig. 1 and Table 2).

Table 1. The world's 29 largest megacities, listed by population (2010) in decreasing order, including latitude, longitude, available LST data and population size. Note: The 10 largest megacities in the Integrated Asian Monsoon Region are indicated in bold; and NA = not available.

	Country	City	Continent	Lat (deg)	Lon (deg)	LST Data MODIS 8-d, 1 km	Pop (mil)
1	Japan	Tokyo	Asia	35.43	139.4	2003-2014	34.6
2	China	Guangzhou	Asia	23.11	113.25	2003-2014	26.3
3	Indonesia	Jakarta	Asia	-6.17	106.82	NA	25.8
4	China	Shanghai	Asia	31.23	121.47	2003-2014	25.8
5	Republic of Korea	Seoul	Asia	37.56	126.99	2003-2014	25.6
6	Mexico	Mexico City	North America	19.50	-99.11	NA	23.5
7	India	Delhi	Asia	28.66	77.21	2003-2008 nighttime	23.5
8	Pakistan	Karachi	Asia	24.86	67.05	2003-2011	22.1
9	Philippines	Quezon City	Asia	14.63	121.03	NA	21.8
10	United States of America	New York	North America	40.70	-73.91	NA	21.5
11	Brazil	São Paulo	South America	-23.53	-46.61	NA	21.3
12	India	Mumbai	Asia	18.96	72.82	NA	21.1
13	United States of America	Los Angeles	North America	34.08	-118.37	NA	17.1
14	Japan	Osaka	Asia	34.66	135.50	2003-2014	16.8
15	China	Beijing	Asia	39.90	116.38	2003-2014	16.7
16	Russia	Moscow	Europe	55.75	37.61	NA	16.2
17	Egypt	Cairo	Africa	30.05	31.25	NA	15.9
18	Bangladesh	Dhaka	Asia	23.72	90.40	2003-2013 nighttime	15.9
19	India	Kolkata	Asia	22.56	88.36	2003-2014 nighttime	15.8
20	Argentina	Buenos Aires	South America	-5.26	-79.96	NA	14.4
21	Thailand	Bangkok	Asia	13.750	100.517	NA	14.2
22	Turkey	Istanbul	Asia	41.019	28.965	NA	13.7
23	Iran	Tehran	Asia	35.672	51.424	NA	13.7
24	United Kingdom	London	Europe	51.500	-0.117	NA	13.2
25	Nigeria	Lagos	Africa	6.453	3.396	NA	13.0
26	Brazil	Rio de Janeiro	South America	-22.900	-43.233	NA	12.8
27	France	Paris	Europe	48.867	2.333	NA	10.6
28	China	Shenzhen	Asia	22.544	114.110	NA	10.0
29	China	Tianjin	Asia	39.128	117.185	NA	10.0

4. RESULTS

4.1. The Surface Urban Heat Island 1 km Resolution Cross-Sections

First, the cross-sections of LST for 10 selected megacities according to the latitude (E-W) as shown in Figs. (2, 4) and longitude (N-S) Figs. (3, 5) of their SUHI averaged for 2003-2014 period, were investigated. The exact location of the city center was taken from Brinkhoff [46] and confirmed by Google Earth.

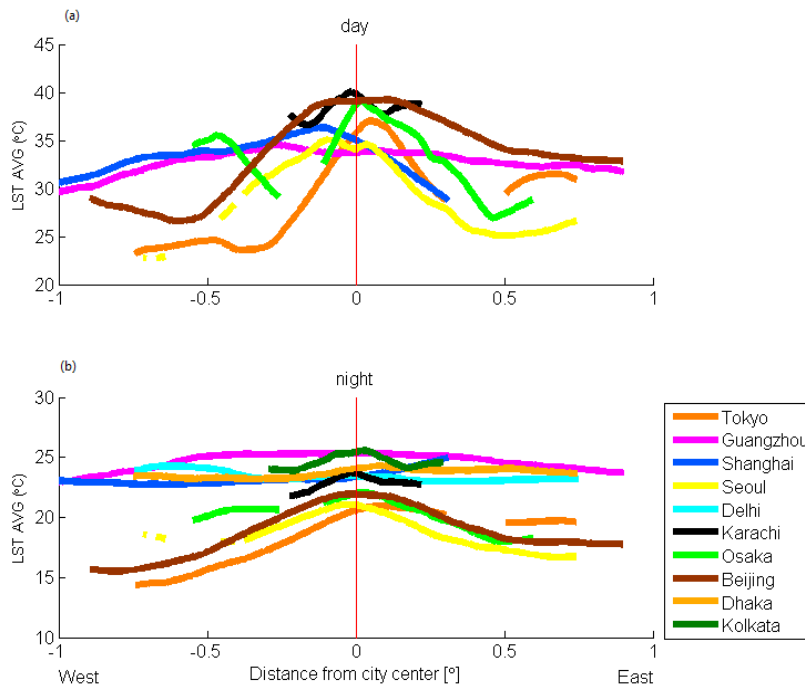


Fig. (2). Latitudinal distribution of 12-year (2003-2014) mean LST for (a) daytime and (b) nighttime, based on 1 km Aqua -MODIS. The 10 Asian megacities are listed on the panel to the right. Data are limited in time-span for Karachi (up to 2011), Dhaka (up to 2013), Delhi (up to 2008) and Kolkata (nighttime only).

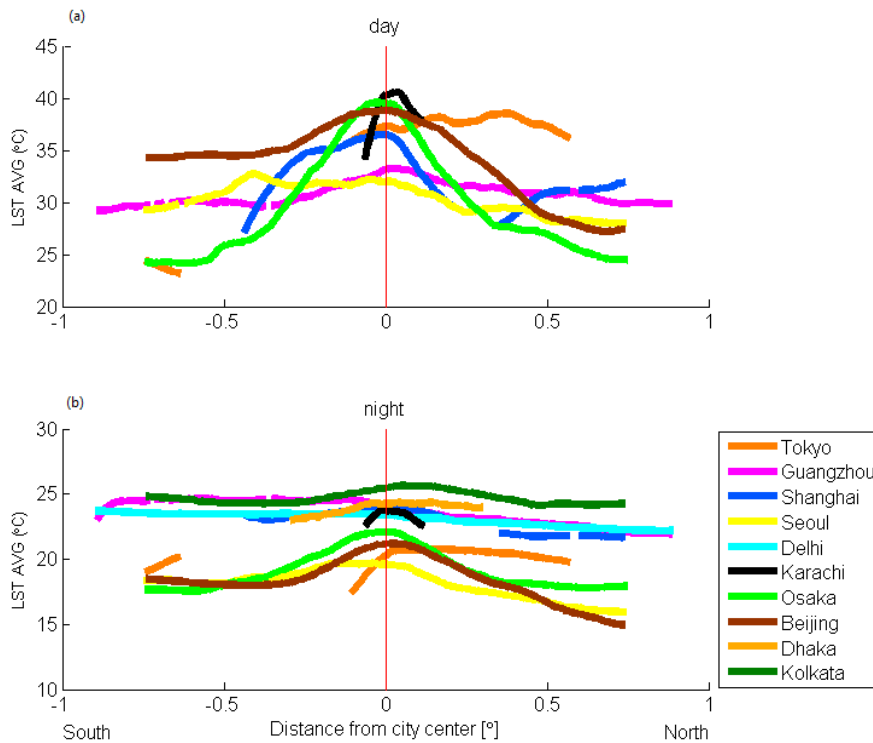
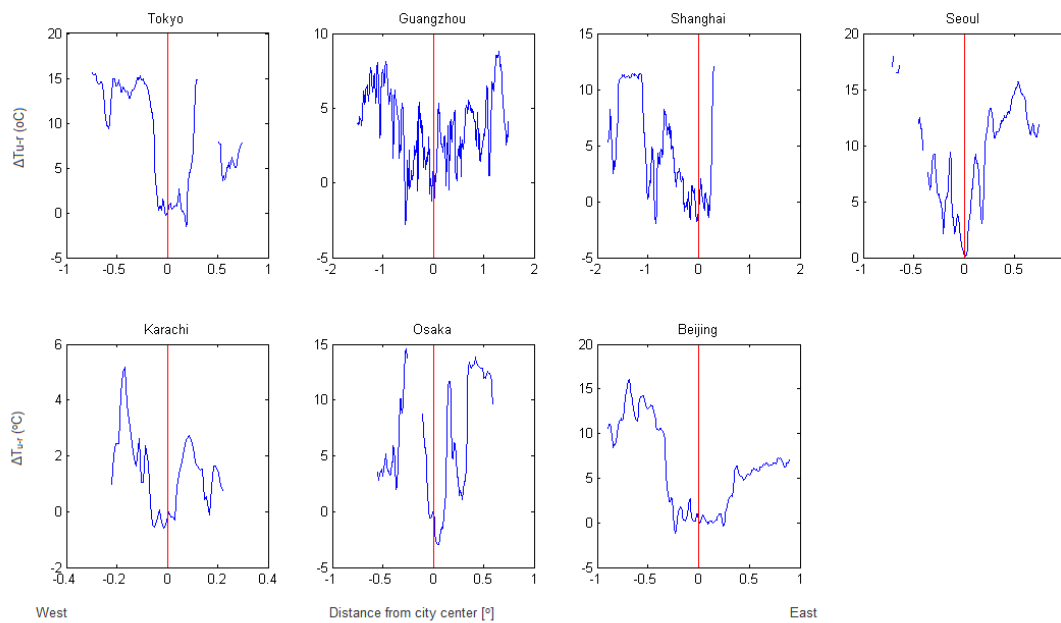


Fig. (3). As in Fig. (2) but for the longitudinal distributions.

(a) Latitudinal distribution of 12-year mean during daytime



(b) Latitudinal distribution of 12-year mean during nighttime

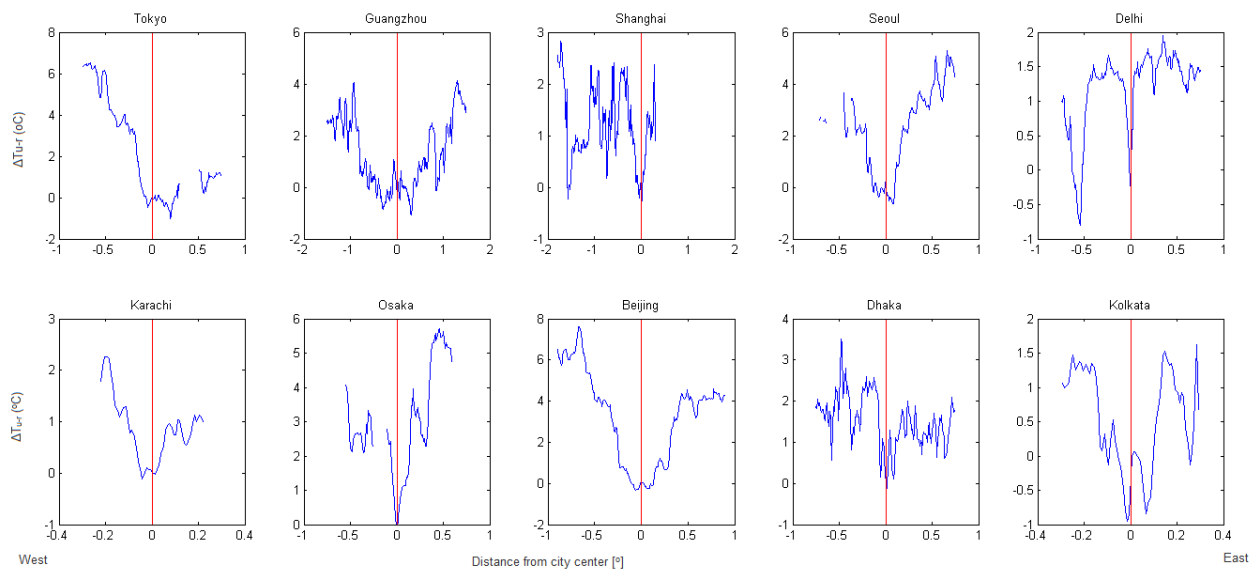


Fig (4). The change in Urban-Rural of the longitudinal distribution of 12-year mean (a) daytime and (b) nighttime LST based on Aqua -MODIS data sets for 1 km for each megacity.

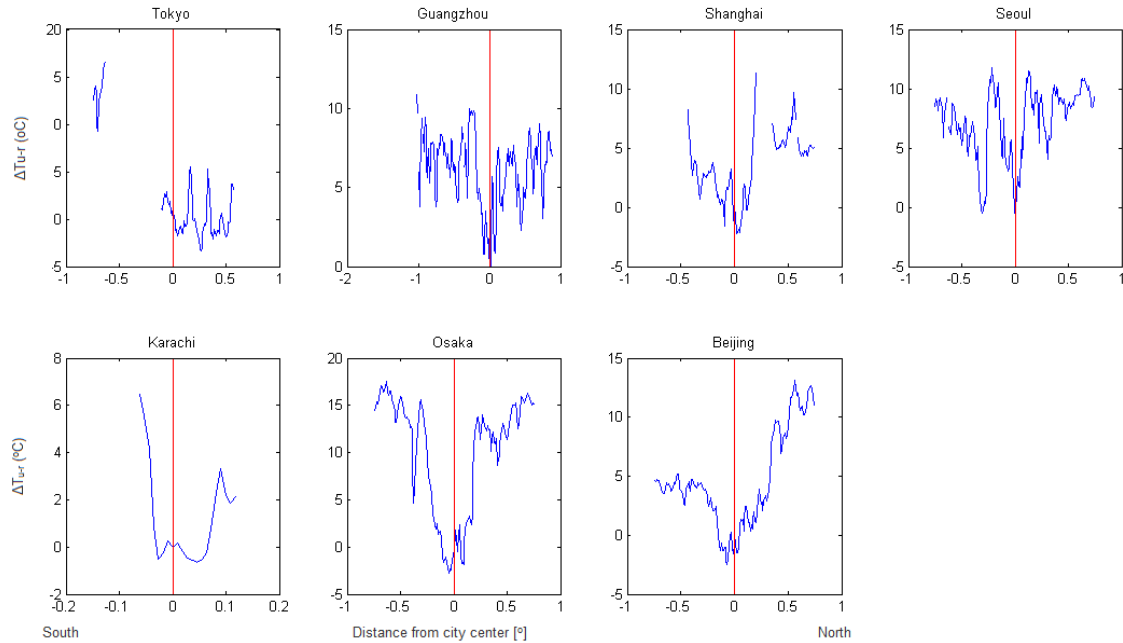
Figs. (2, 3) compare the Lat and Lon distributions of the SUHI Aqua -MODIS LSTs in the proximity of the city centers. They show that the LSTs are on the average decreasing with distance with an approximated bell-shaped distribution for both day and night, with a pronounced SUHI maximum over the city center. However, it should be noted that our figures are averages over a period of 12-y during which the city fringes have probably undergone significant LST changes. Hence the LST decreases with distance from city center represent a 12-y average picture which misses sub-period variations.

It is also interesting to note that during daytime, pronounced maximum LST are found especially over the megacities of Tokyo, Seoul and Beijing with a larger decrease for latitudinal (E-W) variation as shown in Fig. (2a) as compared with the longitudinal (N-S) change in (Fig. 3a).

During nighttime as shown in Figs. (2b, 3b), the LST slopes were found larger in the coldest cities, *i.e.*, Tokyo,

Seoul, Osaka and Beijing (the cities with lower temperatures). In addition, a relatively flat LST distribution along both latitude and longitude was found in Guangzhou, Shanghai, Delhi and Dhaka; it should be noted, however, that SUHI can still reach $\sim 2-4^{\circ}\text{C}$ (as particularly noticed in the individual cities' cross-sections in Figs. (4, 5)). In Shanghai, the flat distribution at night is contrasted during the daytime by a pronounced bell-shaped distribution in both latitude/longitude of $\sim 8-11^{\circ}\text{C}$.

(a) Longitudinal distribution of 12-year mean during daytime



(b) Longitudinal distribution of 12-year mean during nighttime

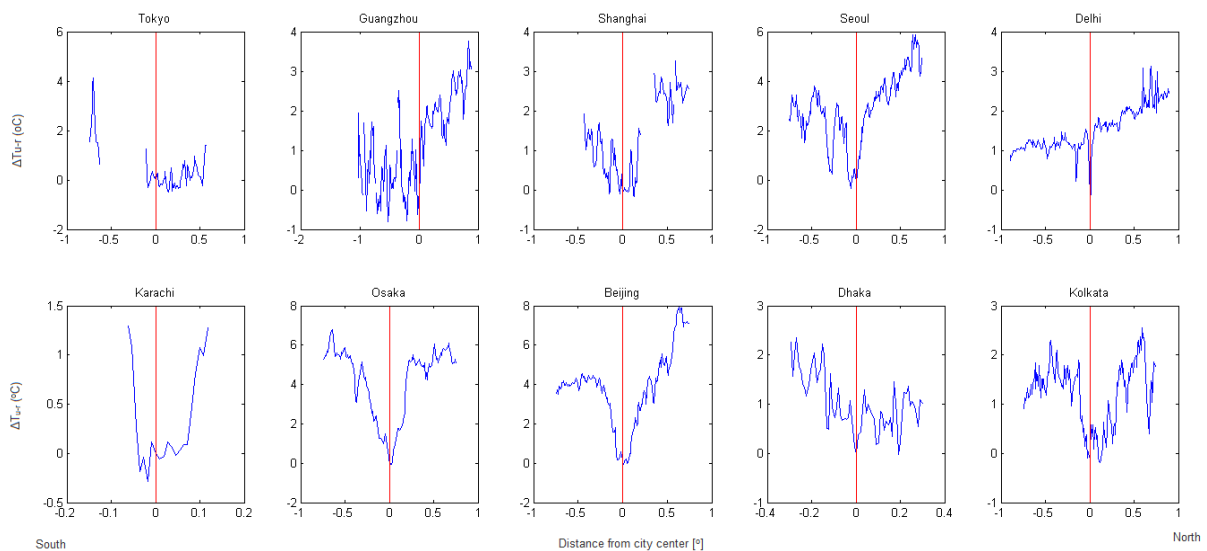


Fig (5). The change in Urban-Rural of the longitudinal distribution of 12-year mean (a) daytime and (b) nighttime LST based on Aqua -MODIS data sets for 1 km for each megacity.

4.1.1. Individual LST Cross-Sections

The “Urban minus Rural temperature” differences, ΔT_{ur} LST Aqua -MODIS data is calculated between the city center and the nearby urban area for each megacity, in terms of latitudinal as in Fig. (4) and longitudinal in Fig. (5) for (a) day and (b) night. In Fig. (4), a pronounced distribution was found in Tokyo, Seoul, Osaka and Beijing (arranged in the decreasing order) with a maximum of 15°C, following with Shanghai (12°C); Guangzhou (8.8°C) and Karachi with 5.1°C SUHI. Fig. (4b) represents the latitude nighttime, the maximum SUHI was found with smaller values (compared to the daytime), in Beijing (7.6°C); Tokyo (6.4°C), Osaka and Seoul (~5.5°C); Guangzhou and Dhaka (~3.5°C). In the other megacities, ΔT_{ur} reaches maximum values of 2.5°C SUHI only.

According to Fig. (5a), for the longitude daytime data, the maximum SUHI found in two cities Osaka and Beijing in the order of 15°C. Following are Seoul, Shanghai and Guangzhou with ~11°C; and Karachi with 6.5°C SUHI. Fig. (5b) represents the longitude nighttime data; the maximum temperature differences were also found to be more moderate compared to the daytime as in Fig. (4). For example, the maximum SUHI was found in Tokyo (6.4°C E-W; 4.1°C N-S), Seoul (5.2°C E-W; 5.9°C N-S), Osaka (5.7°C E-W; 6.7°C N-S) and in Beijing (7.6°C E-W; 7.9°C N-S).

In all the four graphs Figs. (2, 5), it can be identified the location where the SUHI begins, ends and sometimes starts again. For example, Figs. (2, 3) shows the SUHI appears very clearly in Tokyo, Beijing and Osaka during the daytime, while at nighttime the SUHI appears clearly in the tropical megacities of Kolkata and Seoul.

The next section presents maps of the day and night LST trends with time for all global megacities during the periods 2002-2012 and 2003-2014 for Terra and Aqua, respectively.

4.2. Maps of Global Megacities LST Trends with Time

In order to obtain a global map of day and night LST trends based on Terra and Aqua -MODIS temperatures that are covering the largest cities similar to the methodology employed by Alpert [5] for aerosol trends, were employed. However, here the trends were calculated by the LST time-slopes. The maps in Figs. (6, 7) represent the world's 233 largest cities having populations exceeding 2 million [46]. Circles of various diameters and colors indicate the extent and sign of the LST tendencies (see bottom panel). The circles radii represent the value of the LST trends, while the color indicates the sign of the trend, blue/red indicates decrease/increase.

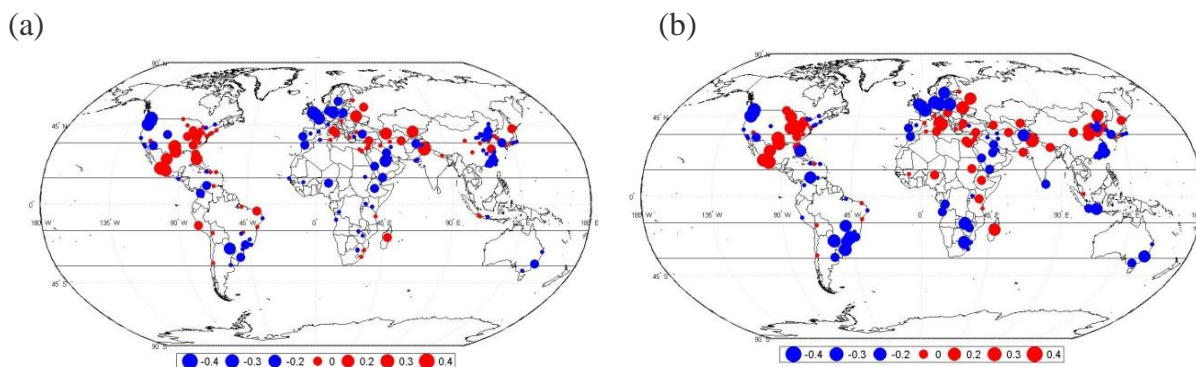


Fig. (6). Global distribution of daytime LST trends for the world's 233 largest cities (populations exceeding 2 million) during the 11-year period 2002-2012, based on LST data sets retrieved from (a) Terra -MODIS (176 cities) and (b) Aqua -MODIS (169 megacities) at $1^\circ \times 1^\circ$ horizontal intervals. Months with cloudiness exceeding 0.7 and cities with less than 6 years of data availability were not included.

Our figures clearly indicate areas where LST slopes are positive or negative during the study period, 2002-2012. The data also reveal the effect of urbanization on LST, with changes associated with a low/high level of anthropogenic development. The global data provided by the two sensors (Aqua/Terra) suggest as follows. The Terra -MODIS shown in Fig. (6a) and Aqua in Fig. (6b) show similar rising LST trends during daytime, were found over the majority of the selected sites in the areas of the Mid-East, the Asian Monsoon region and in the S. & E. of the USA. In contrast, declining LST trends were dominant in Europe, Saudi Arabia, parts of NW America, and the E. part of S. America.

Based on Terra -MODIS data from the 29 megacities (population over 10 million) in the sample, in Fig. (6a) shows a significant LST increase in Asian megacities, *i.e.*, Cairo, Jakarta, Istanbul, Seoul, Tehran, Osaka and especially in Moscow. Increasing LST is also found in Mexico City and New York. In contrast, London and Paris, Los Angeles, São Paulo, Rio de Janeiro and Buenos Aires, and some Asian areas (Tokyo, Beijing, Tianjin and Karachi), exhibit declining LSTs. Out of the 29 megacities Terra and Aqua -MODIS ($1^{\circ}\times 1^{\circ}$) show similar increasing trends in Cairo, Istanbul, Osaka and Moscow. Similar declining LSTs were found for both Terra/Aqua in London, Paris, Los Angeles, São Paulo, Rio de Janeiro, Buenos Aires and Tokyo (Fig. 6 and Table 2).

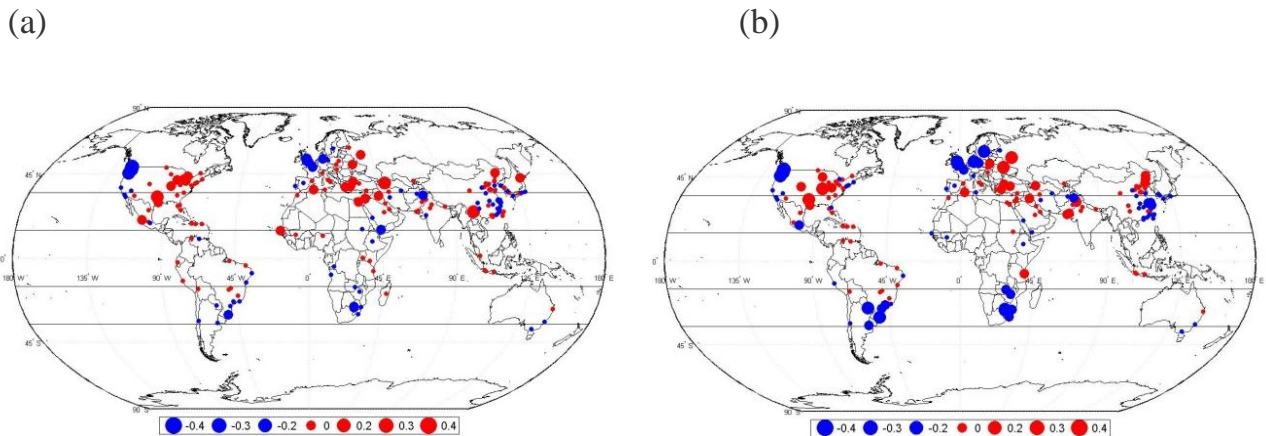


Fig.(7). As in Fig. (6) but for nighttime based on LST data sets of (a) Terra -MODIS (179 cities) and (b) Aqua -MODIS (172 megacities) at $1^{\circ}\times 1^{\circ}$.

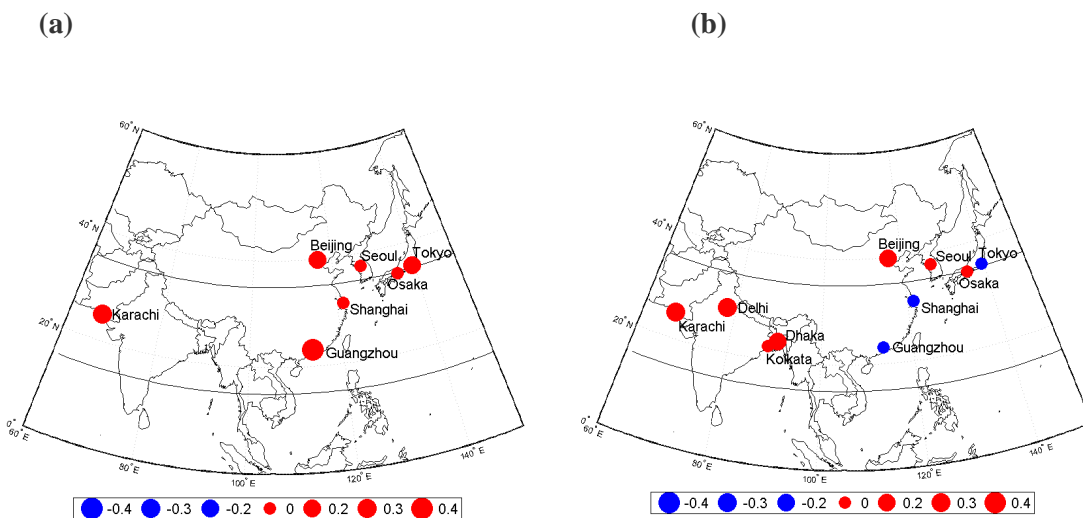


Fig. (8). Aqua -MODIS LST trends during daytime (a-left panel) and nighttime (b-right panel), for the June-August during 2003-2014, based on 1 km Aqua -MODIS. Note that blue/red color indicates negative/positive trends. Cities with incomplete data are Karachi (2002-2011), Dhaka (2002-2013), Delhi (2002-2008) and Kolkata (no daytime records).

The 10 megacities LST trends in Fig. (8) and Table (3) (based on Aqua -MODIS) are more pronounced due to the 1 km resolution as compared with the previous maps at $1^{\circ}\times 1^{\circ}$ in Figs. (6, 7). The Aqua -MODIS results for the Monsoon Asian Region clearly show dominant increasing LSTs during daytime. Furthermore, declining nighttime LST was indicated in the three largest megacities, *i.e.*, Tokyo, Guangzhou and Shanghai. The Daily Temperature Range (DTR) was found to increase except for Osaka. In addition, increases in the LST throughout the day and night were found in Seoul, Karachi, Osaka and Beijing. Our statistical estimates for the slopes during daytime hours were found to be significant at the 95% confidence level ($p < 0.05$) only for Karachi ($p < 0.03$). Note that the Karachi data are for 11 years only, ending in 2011; (Table 3).

Table 2. The world's top 29 megacities, listed by number of inhabitants in decreasing order (see Table 1). The 2002–2012 LST trends (°C/11y) are for the two MODIS sensors, Terra and Aqua, at 1°×1°; NA = not available. Statistically significant slopes at a 95% (*i.e.*, $P < 0.05$). In parentheses, the (R^2 ; P -value) are also indicated.

The top 29 Largest Megacities			Terra -MODIS Trend		Aqua -MODIS Trend	
			Day	Night	Day	Night
1	Japan	Tokyo	-0.049 (0.2944; 0.2660)	-0.048 (0.1535; 0.5142)	-0.06 (0.1897; 0.4636)	NA
2	China	Guangzhou	NA	0.093 (0.1708; 0.4892)	NA	NA
3	Indonesia	Jakarta	0.067 (0.2126; 0.1798)	0.095 (0.4065; 0.0473)	-0.03 (0.0402; 0.5788)	0.052 (0.1971; 0.1987)
4	China	Shanghai	NA	-0.045 (0.0665; 0.4719)	NA	-0.129 (0.3545; 0.1584)
5	Republic of Korea	Seoul	0.054 (0.0749; 0.4154)	0.016 (0.0067; 0.8111)	-0.01 (0.0012; 0.9249)	NA
6	Mexico	Mexico City	0.064 (0.0128; 0.7403)	0.07 (0.1157; 0.3704)	0.23 (0.1411; 0.2847)	0.056 (0.2686; 0.1249)
7	India	Delhi	NA	0.023 (0.0280; 0.6226)	NA	0.067 (0.1514; 0.2369)
8	Pakistan	Karachi	-0.001 (0.0000; 0.9921)	0.028 (0.0086; 0.7867)	0.10 (0.0429; 0.5411)	0.119 (0.1425; 0.2524)
9	Philippines	Quezon City	NA	NA	NA	NA
10	United States of America	New York	0.016 (0.0041; 0.8515)	0.012 (0.0044; 0.8461)	-0.03 (0.0067; 0.8104)	0.005 (0.0006; 0.9414)
11	Brazil	São Paulo	-0.094 (0.1943; 0.1748)	-0.058 (0.0983; 0.3478)	-0.20 (0.2331; 0.1326)	-0.114 (0.1351; 0.2661)
12	India	Mumbai	NA	NA	NA	NA
13	United States of America	Los Angeles	-0.03 (0.0134; 0.7344)	-0.049 (0.0800; 0.3994)	-0.03 (0.0196; 0.6810)	-0.062 (0.1315; 0.2731)
14	Japan	Osaka	0.005 (0.0007; 0.9445)	0.088 (0.2444; 0.2130)	0.05 (0.0726; 0.4833)	-0.086 (0.2148; 0.4318)
15	China	Beijing	-0.048 (0.0164; 0.7075)	0.042 (0.0782; 0.4050)	0.04 (0.0139; 0.7299)	0.024 (0.0364; 0.5741)
16	Russia	Moscow	0.183 (0.0803; 0.3985)	0.188 (0.2729; 0.0992)	0.30 (0.2123; 0.1538)	0.272 (0.4365; 0.0269)
17	Egypt	Cairo	0.099 (0.3589; 0.0515)	0.10 (0.4261; 0.0295)	0.19 (0.4963; 0.0155)	0.078 (0.2730; 0.0992)
18	Bangladesh	Dhaka	NA	NA	NA	NA
19	India	Kolkata	NA	NA	NA	NA
20	Argentina	Buenos Aires	-0.03 (0.0126; 0.7425)	-0.071 (0.0617; 0.4613)	-0.16 (0.1605; 0.2221)	-0.194 (0.2542; 0.1138)
21	Thailand	Bangkok	NA	NA	NA	NA
22	Turkey	Istanbul	0.062 (0.0431; 0.5403)	0.146 (0.3246; 0.0673)	0.12 (0.1123; 0.3137)	0.135 (0.2502; 0.1171)
23	Iran	Tehran	0.027 (0.0052; 0.8331)	0.093 (0.1002; 0.3429)	-0.05 (0.0157; 0.7133)	0.051 (0.0336; 0.5896)
24	United Kingdom	London	-0.269 (0.3019; 0.0800)	-0.142 (0.4567; 0.0224)	-0.30 (0.4102; 0.0460)	-0.191 (0.6933; 0.0015)
25	Nigeria	Lagos	NA	NA	NA	NA
26	Brazil	Rio de Janeiro	-0.089 (0.1744; 0.2013)	-0.039 (0.0492; 0.5120)	-0.20 (0.2543; 0.1137)	-0.076 (0.1068; 0.3267)
27	France	Paris	-0.256 (0.3255; 0.0668)	-0.166 (0.3162; 0.0718)	-0.32 (0.5257; 0.0177)	-0.188 (0.5331; 0.0107)
28	China	Shenzhen	NA	0.092 (0.1633; 0.3686)	-0.09 (0.1106; 0.4209)	-0.001 (0.0002; 0.9812)
29	China	Tianjin	-0.044 (0.0588; 0.4725)	0.058 (0.3035; 0.0790)	0.11 (0.1523; 0.2353)	0.033 (0.0862; 0.4102)

Note: The top 10 megacities in the Monsoon Asian Integrated Region are indicated in bold.

Table 3. The 10 megacities in the Asian Monsoon Region; LST slope (°C/12y) during June-August 2003-2014, based on 1 km Aqua -MODIS. Statistically significant slopes at a 95% (*i.e.* $P < 0.05$) are in bold. NA = not available.

City	R ²		P- Value		Trend		
	Day	Night	Day	Night	Day	Night	Δ (DTR)
Tokyo	0.0534	7.09E-05	0.4695	0.9792	0.113	-0.002	0.117
Guangzhou	0.1808	0.0308	0.2205	0.5852	0.305	-0.024	0.329
Shanghai	0.0107	0.0413	0.7487	0.5261	0.051	-0.046	0.097
Seoul	0.0718	0.0335	0.3995	0.5689	0.095	0.053	0.042
Delhi (until 2008)**	NA	0.4830	NA	0.1253	NA	0.211	NA
Karachi (until 2011)**	0.4142	0.3238	0.0326	0.0676	0.243	0.218	0.025
Osaka	0.0018	0.0233	0.8948	0.6352	0.018	0.039	-0.021
Beijing	0.2600	0.3029	0.0903	0.0637	0.110	0.108	0.002
Dhaka (until 2013)**	NA	0.0735	NA	0.3938	NA	0.147	NA
Kolkata**	NA	0.0266	NA	0.6123	NA	0.058	NA

Note: **Data for Karachi, Dhaka, Delhi and Kolkata are limited as indicated earlier.

5. DISCUSSION

According to the report issued by the UN's Department of Economic and Social Affairs [1], the world's human population is expected to exceed 10 billion in the near future. Countries with high population densities will consequently witness rising pressure on the environment. The pressure in the Asian region is likely to increase even more when compared to other countries due to the rising demand for grains and economic development [9].

Since the beginning of the 21st century, most studies have examined climate change with in-situ data, usually collected in one or two cities [20, 51]. Here, in contrast, the use of latitudinal and longitudinal cross-sectional Aqua -MODIS LST data enabled mapping of 10 Asian megacities during June-August. Based on these data, we found that the sites exhibiting maximum SUHI intensity roughly coincided with the heavily built-up areas located in major city centers. Hence, cities with extremely urbanized areas, characterized by low albedo and dense construction, exhibited significantly higher daytime surface temperatures when compared to the surrounding rural area comprised of relatively moister vegetated areas [20]. With respect to the LST magnitudes shown in Figs. (4, 5), steeper temperature gradients were observed during daytime hours, *i.e.*, Tokyo, Seoul, Osaka and Beijing with 15°C gradients, followed by Shanghai with 12°C and Guangzhou with 8.8° C. This finding fit those in the Tran *et al.* [20] study, which produced a similar ordering of cities by temperature gradient, *i.e.*, Tokyo, followed by Beijing, Seoul and Shanghai. Temperatures were also found to decrease outward from the city center, distributed according to an approximate bell-shaped curve during the day, a finding that can be explained by the UHI phenomenon. During the night, megacities such as Guangzhou and Shanghai showed far gentler SUHI, which can be explained by the effect of peripheral cities or industrial centers, a condition that influences LST. Another factor could be the sun insolation that plays an important contribution to the increase of daily SUHI. Tran *et al.* [21] also suggested that SUHI diurnal variations are due to differences in urban-rural characteristics such as moisture availability and surface cooling rates, further affected by topography, rural surroundings and the geographic location of cities relative to the sea [20, 52].

In contrast to in-situ UHI studies, in which minimum daily temperatures tend to increase at a higher rate than do daily temperatures (the latter inducing a decreasing long-term diurnal temperature range; see for example [52, 53]), the satellite-based SUHIs temperatures observed tending to be higher during the day, with peak temperatures reached in areas of large buildings or paved surfaces, and lowest during the night, due to difference in surface properties and cooling rates [20, 51]. Therefore, in the current study, in order to monitor the seasonal variations in SUHIs (at a 1 km resolution), we focused only on Aqua -MODIS rather than Terra data, thus ensuring that the satellite sensors could differentiate between LST trends observed in megacities and those observed in the surrounding rural areas, both at 13:30 local time (LT), frequently observed to be the hottest hour of the day (as opposed to the 10:30 LT Terra measurement). Here, the DTR increased during 2002-2014 Table (3), which fit the earlier findings reported by Roth [51] and Tran [20], among others. Throughout the research period, a negative DTR was found only in Osaka. Furthermore, according to the IPCC's Atmosphere-Ocean Global Climate Model (OGCM) simulations the DTR will increase over central Asia and be significantly higher there than in other regions during the summer months of the 2050s and 2080s [54 - 56].

We should stress that, as Roth [57] has already noted, the limited range of urban morphologies characterizing the

cities, as well as the role of building density and materials, prevented detailed exploration of temperature trends. Hence, further study is required in order to explore the contribution of these and other parameters, such as population density, energy consumption, and transportation volume, to urban warming.

CONCLUSION

This article has stressed the advantages provided by satellite remote sensing monitoring techniques when performing quantitative climatic observations worldwide, an ability that has significantly enhanced our ability to identify long-term trends in climate change [41]. These techniques have made reliable high-quality global coverage at high spatial resolution available, thereby creating opportunities for researchers to easily obtain improved global meteorological data and thus providing significant advantage relative to ground-based measurements. We should recall, however, that unlike ground-based measurements, satellite data are limited regarding the parameters to be measured; they likewise cannot provide accurate information on climate variables, which are important for the construction of human comfort indices.

The 1 km LST data from Aqua -MODIS can distinguish urban from surrounding rural areas, information supporting statistical analyses by making it possible to create bell-shaped data distributions (for latitude as well longitude magnitudes), which can indicate changes of trends in LST. By doing so, satellites provide us with the opportunity to compare global-temperature trends in different cities on the basis of data obtained from the same source and with the same measurement technology, irrespective of city size.

The same Aqua -MODIS (1 km) satellite source indicates that for Asia's three largest megacities -- Tokyo, Guangzhou and Shanghai -- a recent decrease in nighttime LST trends (2002-2014) has been observed. In contrast, the LST slope for both day and night was found to increase in Seoul, Karachi, Osaka and Beijing. Further research on the physical, economical, and social environment is required in order to better understand and evaluate climate change-induced vulnerabilities in the Asian Monsoon Region. These data are also relevant for assessing the feasibility of introducing adaptation measures in other regions. We should also anticipate that given the vital roles played by surface water and groundwater resources in forestry, agriculture, fisheries, livestock production and industrial activity in the Asian countries, the agricultural sector will continue to be highly sensitive to climate change impacts in that region [4].

As to the Terra -MODIS and Aqua -MODIS ($1^\circ \times 1^\circ$) LST trends, Alpert *et al.* [5] have suggested that in cases where the different sensors show similar trends, the results can be considered reliable. This conclusion is supported by our findings for daytime hours, which were observed as increasing in the Mid-East and the Asian Monsoon region and in the southeastern US during 2002-2012. In contrast, trends in declining LST appeared to be dominant in Europe sites, Saudi Arabia, parts of Northwest America, and the Eastern segment part of South America. One suggestion is that those cities are aware of climate change, therefore implement climate change issues into their policies.

In general, we concluded that the MODIS satellite can be better-utilized if we were to adapt our current technologies and devise new methodologies. While most climatological studies conducted to date have employed in-situ data, the current study incorporated satellite data having global spatial coverage despite being limited in the variables to be observed. Furthermore, despite the methodological limitations of the current study, we suggest that the optimal direction of future research to involve: (a) Obtaining data with higher resolution MODIS 8-day 1 km LST for additional regions; (b) Expanding the list of variables, *e.g.*, air humidity and wind speed, as tracked from land-based meteorological stations; and (c) Applying further combinations of high resolution satellite data with Global Climate Model (GCM) data for evaluation.

ETHICS APPROVAL AND CONSENT TO PARTICIPATE

Not applicable.

HUMAN AND ANIMAL RIGHTS

No Animals/Humans were used for studies that are base of this research.

CONSENT FOR PUBLICATION

Not applicable.

CONFLICT OF INTEREST

The authors declare no conflict of interest, financial or otherwise.

ACKNOWLEDGEMENTS

The authors thank Mr. Tomer Mayan for his assistance and construction of the maps. This research was funded through the international Virtual Institute DESERVE (Dead Sea Research Venue), funded by the German Helmholtz Association and the Gordon Center for Energy Studies. This study was made possible through the generous support of the Porter School of Environmental Studies, Tel Aviv University.

REFERENCES

- [1] United Nations, Department of Economic and Social Affairs, Population Division. World Population Prospects. World Population Prospects (2011 Revision): New York. 2010.
- [2] Molina MJ, Molina LT. Megacities and atmospheric pollution. *J Air Waste Manag Assoc* 2004; 54(6): 644-80. [<http://dx.doi.org/10.1080/10473289.2004.10470936>] [PMID: 15242147]
- [3] United Nations Population Fund (UNFPA). Growing up urban. New York.: Supplement to the State of World Population 2007.
- [4] Solomon S, Ed. Climate change: The physical science basis. New York.: Working Group I, contribution to the fourth assessment report of the IPCC 2007.
- [5] Alpert P, Shvainshtein O, Kishcha P. AOD trends over megacities based on space monitoring using MODIS and MISR. *AJJC* 2012; 1(03): 117-31.
- [6] Dhorde A, Dhorde A, Gadgil AS. Long-term temperature trends at four largest cities of India during the twentieth century. *J Indian Geophys Unio* 2009; 13(2): 85-97.
- [7] Mage D, Ozolins G, Peterson P, et al. Urban air pollution in megacities of the world. *Atmos Environ* 1996; 30(5): 681-6. [[http://dx.doi.org/10.1016/1352-2310\(95\)00219-7](http://dx.doi.org/10.1016/1352-2310(95)00219-7)]
- [8] ADB (Asian Development Bank). Key Indicators <http://www.adb.org> 2002.
- [9] Zeqiang F, Yunlong C, Youxiao Y, Erfu D. Research on the relationship of cultivated land change and food security in China. *Ziran Ziyuan Xuebao* 2001; 16(4): 313-9.
- [10] Lelieveld J, Proestos Y, Hadjinicolaou P, Tanarhte M, Tyrlis E, Zittis G. Strongly increasing heat extremes in the Middle East and North Africa (MENA) in the 21st century. *Clim Chang* 2015; pp. 1-16.
- [11] Pal JS, Eltahir EA. Future temperature in southwest Asia projected to exceed a threshold for human adaptability. *Nat Clim Chang* 2015; 6: 197-200.
- [12] Grimmond CS, Roth M, Oke TR, et al. Climate and more sustainable cities: Climate information for improved planning and management of cities (producers/capabilities perspective). *Procedia Environ Sci* 2010; 1: 247-74. [<http://dx.doi.org/10.1016/j.proenv.2010.09.016>]
- [13] Mills G, Cleugh H, Emmanuel R, et al. Climate information for improved planning and management of mega cities (needs perspective). *Procedia Environ Sci* 2010; 1: 228-46. [<http://dx.doi.org/10.1016/j.proenv.2010.09.015>]
- [14] Clinton N, Gong P. MODIS detected surface urban heat islands and sinks: Global locations and controls. *Remote Sens Environ* 2013; 134: 294-304. [<http://dx.doi.org/10.1016/j.rse.2013.03.008>]
- [15] Fujibe F. Detection of urban warming in recent temperature trends in Japan. *Int J Climatol* 2009; 29(12): 1811-22. [<http://dx.doi.org/10.1002/joc.1822>]
- [16] Fujibe F. Urban warming in Japanese cities and its relation to climate change monitoring. *Int J Climatol* 2011; 31(2): 162-73. [<http://dx.doi.org/10.1002/joc.2142>]
- [17] Itzhak-Ben-Shalom H, Samuels R, Potchter O, Alpert P. Recent trends and future predictions until 2060 of urban warming in four Israeli cities employing the RegCM climate model. *AJJC* 2016; 5(04): 464.
- [18] Potchter O, Itzhak-Ben-Shalom H. Urban warming and global warming: Combined effect on thermal discomfort in the desert city of Beer Sheva, Israel. *J Arid Environ* 2013; 98: 113-22. [<http://dx.doi.org/10.1016/j.jaridenv.2013.08.006>]
- [19] Thorsson S, Lindberg F, Björklund J, Holmer B, Rayner D. Potential changes in outdoor thermal comfort conditions in Gothenburg, Sweden due to climate change: The influence of urban geometry. *Int J Climatol* 2011; 31(2): 324-35. [<http://dx.doi.org/10.1002/joc.2231>]
- [20] Tran H, Uchihama D, Ochi S, Yasuoka Y. Assessment with satellite data of the urban heat island effects in Asian mega cities. *Int J Appl Earth Obs* 2006; 8(1): 34-48. [<http://dx.doi.org/10.1016/j.jag.2005.05.003>]

- [21] Gallo KP, McNab AL, Karl TR, Brown JF, Hood JJ, Tarpley JD. The use of a vegetation index for assessment of the urban heat island effect. *Remote Sens* 1993; 14(11): 2223-30. [http://dx.doi.org/10.1080/01431169308954031]
- [22] Gallo KP, Owen TW. Assessment of urban heat islands: A multi-sensor perspective for the Dallas-Ft. Worth, USA region. *Geocarto Int* 1998; 13(4): 35-41. [http://dx.doi.org/10.1080/10106049809354662]
- [23] Weng Q, Lu D, Schubring J. Estimation of land surface temperature: Vegetation abundance relationship for urban heat island studies. *Remote Sens Environ* 2004; 89(4): 467-83. [http://dx.doi.org/10.1016/j.rse.2003.11.005]
- [24] van Wijngaarden WA, Mouraviev A. Seasonal and annual trends in Australian minimum/maximum daily temperatures. *TOASJ* 2016; 10(1): 39-55. [http://dx.doi.org/10.2174/1874282301610010039]
- [25] Govindankutty M, Chandrasekar A, Bohra AK, George JP, Dasgupta M. The impact of assimilation of MODIS observations using WRF-VAR for the prediction of a monsoon depression during September 2006. *TOASJ* 2008; 2: 68-78. [http://dx.doi.org/10.2174/1874282300802010068]
- [26] Kaufman YJ, Tanré D, Boucher O. A satellite view of aerosols in the climate system. *Nature* 2002; 419(6903): 215-23. [http://dx.doi.org/10.1038/nature01091] [PMID: 12226676]
- [27] Kou X, Jiang L, Bo Y, Yan S, Chai L. Estimation of land surface temperature through blending MODIS and AMSR-E data with the Bayesian maximum entropy method. *Remote Sens* 2016; 8(2): 105. [http://dx.doi.org/10.3390/rs8020105]
- [28] Zhao S, Zhou D, Liu S. Data concurrency is required for estimating urban heat island intensity. *Environ Pollut* 2016; 208(Pt A): 118-24. [http://dx.doi.org/10.1016/j.envpol.2015.07.037] [PMID: 26243476]
- [29] Liu K, Su H, Li X, Wang W, Yang L, Liang H. Quantifying spatial-temporal pattern of urban heat island in Beijing: An improved assessment using land surface temperature (LST) time series observations from LANDSAT, MODIS, and Chinese new satellite GaoFen-1. *IEEE J-Stars* 2016; 9(5): 2028-42.
- [30] Tan M, Li X. Quantifying the effects of settlement size on urban heat islands in fairly uniform geographic areas. *Habitat Int* 2015; 49: 100-6. [http://dx.doi.org/10.1016/j.habitatint.2015.05.013]
- [31] Swain D, Roberts GJ, Dash J, Vinoj V, Lekshmi K, Tripathy S. Impact of rapid urbanization on the microclimate of Indian cities: A case study for the city of Bhubaneswar. *Proceedings, SPIE Asia-Pacific Remote Sensing Conference*. 2016; 98772X.
- [32] Elhacham E, Alpert P. Impact of coastline-intensive anthropogenic activities on the atmosphere from moderate resolution imaging spectroradiometer (MODIS) data in Dubai (2001–2014). *Earths Futur* 2016; 4(3): 54-61. [http://dx.doi.org/10.1002/2015EF000325]
- [33] Zhuo H, Liu Y, Jin J. Improvement of land surface temperature simulation over the Tibetan Plateau and the associated impact on circulation in East Asia. *Atmos Sci Lett* 2016; 17(2): 162-8. [http://dx.doi.org/10.1002/asl.638]
- [34] Zhou C, Wang K. Land surface temperature over global deserts: Means, variability, and trends. *J Geophys Res Atmos* 2016; 121(14): 344-57.
- [35] Lensky IM, Dayan U. Satellite observations of land surface temperature patterns induced by synoptic circulation. *Int J Climatol* 2015; 35(2): 189-95. [http://dx.doi.org/10.1002/joc.3971]
- [36] Martínez D, Jiménez MA, Cuxart J, Mahrt L. Heterogeneous nocturnal cooling in a large basin under very stable conditions. *Boundary-Layer Meteorol* 2010; 137(1): 97-113. [http://dx.doi.org/10.1007/s10546-010-9522-z]
- [37] Lensky IM, Dayan U. Detection of fine-scale climatic features from satellites and implications for agricultural planning. *Bull Am Meteorol Soc* 2011; 92(9): 1131-6. [http://dx.doi.org/10.1175/2011BAMS3160.1]
- [38] Holtslag AA, Svensson G, Baas P, *et al.* Stable atmospheric boundary layers and diurnal cycles: Challenges for weather and climate models. *Bull Am Meteorol Soc* 2013; 94(11): 1691-706. [http://dx.doi.org/10.1175/BAMS-D-11-00187.1]
- [39] Jin M, Dickinson RE. Land surface skin temperature climatology: Benefitting from the strengths of satellite observations. *Environ Res Lett* 2010; 5(4): 044004. [http://dx.doi.org/10.1088/1748-9326/5/4/044004]
- [40] Kloog I, Chudnovsky A, Koutrakis P, Schwartz J. Temporal and spatial assessments of minimum air temperature using satellite surface temperature measurements in Massachusetts, USA. *Sci Total Environ* 2012; 432: 85-92. [http://dx.doi.org/10.1016/j.scitotenv.2012.05.095] [PMID: 22721687]
- [41] Zhu W, Lú A, Jia S. Estimation of daily maximum and minimum air temperature using MODIS land surface temperature products. *Remote Sens Environ* 2013; 130: 62-73. [http://dx.doi.org/10.1016/j.rse.2012.10.034]

- [42] Kilibarda M, Hengl T, Heuvelink G, *et al.* Spatio-temporal interpolation of daily temperatures for global land areas at 1 km resolution. *J Geophys Res Atmos* 2014; 119(5): 2294-313. [<http://dx.doi.org/10.1002/2013JD020803>]
- [43] Blandford TR, Humes KS, Harshburger BJ, Moore BC, Walden VP, Ye H. Seasonal and synoptic variations in near-surface air temperature lapse rates in a mountainous basin. *J Appl Meteorol Climatol* 2008; 47: 249-61. [<http://dx.doi.org/10.1175/2007JAMC1565.1>]
- [44] Imhoff ML, Zhang P, Wolfe RE, Bounoua L. Remote sensing of the urban heat island effect across biomes in the continental USA. *Remote Sens Environ* 2010; 114: 504-13. [<http://dx.doi.org/10.1016/j.rse.2009.10.008>]
- [45] Peng S, Piao S, Ciais P, *et al.* Surface urban heat island across 419 global big cities. *Environ Sci Technol* 2012; 46(2): 696-703. [<http://dx.doi.org/10.1021/es2030438>] [PMID: 22142232]
- [46] Brinkhoff T. The principal agglomerations of the world 2006. Available at: <http://www.adb.org>[http:// www.citypopulation.de](http://www.citypopulation.de)
- [47] The Moderate Resolution Imaging Spectroradiometer <https://www.nasa.gov/>. Accessed on: 03 April
- [48] Remer LA, Kleidman RG, Levy RC, *et al.* Global aerosol climatology from the MODIS satellite sensors. *J Geophys Res-Atmos* (1984–2012) 2008; 113: D14S07.
- [49] Zhang J, Reid JS, Holben BN. An analysis of potential cloud artifacts in MODIS over ocean aerosol optical thickness products. *Geophys Res Lett* 2005; 32: L15803. [<http://dx.doi.org/10.1029/2005GL023254>]
- [50] The MODIS 8-day 1-km LST. Available at: <https://giovanni.sci.gsfc.nasa.gov/giovanni/> [Accessed on: 03 April 2017].
- [51] Roth M, Oke TR, Emery WJ. Satellite-derived urban heat islands from three coastal cities and the utilization of such data in urban climatology. *Int J Remote Sens* 1989; 10(11): 1699-720. [<http://dx.doi.org/10.1080/01431168908904002>]
- [52] Lebassi B, Gonzalez J, Fabris D, *et al.* Observed 1970-2005 cooling of summer daytime temperatures in coastal California. *J Clim* 2009; 22(13): 3558-73. [<http://dx.doi.org/10.1175/2008JCLI2111.1>]
- [53] Price C, Michaelides S, Pashiardis S, Alpert P. Long term changes in diurnal temperature range in Cyprus. *Atmos Res* 1999; 51(2): 85-98. [[http://dx.doi.org/10.1016/S0169-8095\(99\)00022-8](http://dx.doi.org/10.1016/S0169-8095(99)00022-8)]
- [54] Lal M, Harasawa H. Future climate change scenarios for Asia as inferred from selected coupled atmosphere-ocean global climate models. *J Meteorol Soc Jpn* 2001; 79(1): 219-27. [<http://dx.doi.org/10.2151/jmsj.79.219>]
- [55] Kumar KR, Kumar KK, Pant GB. Diurnal asymmetry of surface temperature trends over India. *Geophys Res Lett* 1994; 21(8): 677-80. [<http://dx.doi.org/10.1029/94GL00007>]
- [56] Yoshino M. Global warming and urban climates: report of the Research Center for Urban Safety and Security, Kobe University Special Report No. 1. Proceedings of the Second Japanese-German Meeting 1998; *Klima Analyse fur die Stadtplanung* 1998; 123-4.
- [57] Roth M. Review of urban climate research in (sub) tropical regions. *Int J Climatol* 2007; 27(14): 1859-73. [<http://dx.doi.org/10.1002/joc.1591>]